Proceedings of the 21st ICSMGE, Vienna, Austria, 14 – 19 June 2026. Pistrol, Adam & Schweiger (eds.)
Published by: ÖGG, Austrian Society for Geomechanics, Salzburg, Austria, ISBN 978-3-9503898-4-5
https://doi.org/10.53243/ICSMGE2026-2086

Numerical modelling of laterally loaded piles driven in calcareous weak rocks

Wan Hei Charles Wong
AtkinsRéalis, Bristol, UK; Formerly School of Civil, Aerospace and Design Engineering, University of Bristol, Bristol, UK; Chareles.Wong@atkinsrealis.com

Tingfa Liu, Andrea Diambra
School of Civil, Aerospace and Design Engineering, University of Bristol, Bristol, UK

Kai Wen
Department of Civil, Maritime and Environmental Engineering, University of Southampton, Southampton, UK

Francesca Ciavaglia
Lloyd's Register, Bristol, UK

ABSTRACT: Weak rocks are increasingly frequently encountered at foundation levels as offshore renewable wind energy development expands into deeper waters and new areas using bottom-fixed and floating wind turbines. In-situ strength and stiffness characteristics of rocks impact profoundly the choices of foundation types and installation methods, which in turn affect the local and global rock-foundation interaction mechanisms and the foundation's serviceability and ultimate capacity. This paper reports how installation effects can be captured explicitly in three-dimensional (3D) finite element (FE) modelling of impact driven piles in calcareous weak rocks by considering layers of materials adjacent to pile shaft and beneath pile base with distinct mechanical properties that capture rock's peak, post-rupture and ultimate states. A general modelling methodology employing simplified constitutive models is presented, with illustrative examples being drawn on from recent studies of laterally loaded driven piles in low- to medium-density chalk and fine- to medium-grained calcarenite. The modelled load-displacement trends and bending moment profiles are benchmarked against field pile test measurements. Local rock-pile interaction is further characterised by distributed lateral pressure against soil displacement (p-y) curves extracted from the FE models and further linked to rock strengths. The overall outcomes enable further development and validation of one-dimensional (1D) beam-spring models for efficient modelling and practical design of lateral loaded piles in weak rocks.

KEYWORDS: Finite element analysis, Installation method, Pile foundations, Rocks

1 INTRODUCTION

Offshore renewable wind energy plays a central role in regional and global endeavours for Net Zero. Rocky seabeds are increasingly frequently encountered as offshore wind farms are being constructed in deeper waters and new development areas in North, Baltic, Celtic and Irish Seas and the coasts of Korea and Japan. Palix (2025) highlighted in the context of French wind farm developments, the geological and mechanical properties of rocks profoundly influence the design choices of monopile, gravity base or jacket foundation types, as well as impact driven, drilled-and-grouted, drive-drill-drive (DDD) and other pile installation methods, posing significant challenges and uncertainties in pile design (Randolph, 2019).

Sedimentary carbonated rocks such as calcarenite and chalk exhibit significant variations and variabilities in their mineralogical, physical and mechanical properties imparted by depositional environment, geological history, natural and induced macro structures and fissures. Their mechanical response can vary from highly brittle to fully ductile, depending critically on the level of cementation, de-structuration and applied stresses. Lagioia & Nova (1995) and Cuccovillo & Coop (1999) reported how inter-particle bonding affected the yielding and strength characteristics of sand-sized calcarenites and how increasing confining pressure triggered the transition from rock-like to soil-like frictional behaviour. Lovera (2019) noted the loss of cohesion in highly compacted and crushed calcarenite materials post pile driving. Liu et al. (2023) reported, from high pressure triaxial compression tests, that low- to medium-density chalk developed a curved strength envelope and an elliptical yield locus indicative of large-scale de-structuration of inter-particle cementation (Figure 1). The results then allowed the determination of Mohr-Coulomb effective strengths at peak, post-rupture and ultimate states (Pedone et al. 2023).

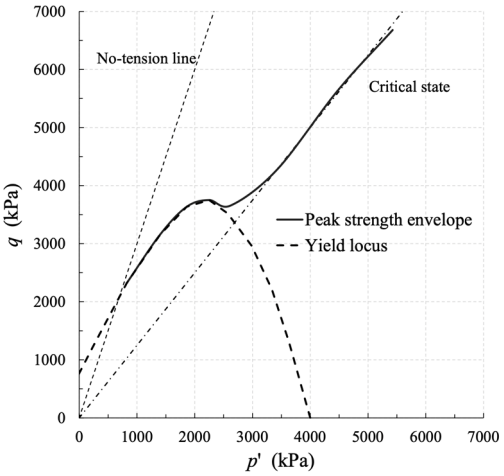

Figure 1. Yield locus and strength envelope for a low- to medium-density chalk from St Nicholas at Wade (SNW, Kent, UK) (modified from Liu et al. (2023)).

High pressure percussive stresses applied under impact hammering of piles into calcareous soft rocks result in de-structuration of inter-particle cementation and crushing of calcium carbonate particles close to pile shaft and beneath base, leading to distinctly low resistances to driving. Subsequent lateral loading to ultimate capacity mobilises larger volumes of rocks at the passive sides and imposes stresses much higher than those at in-situ. Buckley et al. (2018) and Vinck et al. (2025) characterised the installation effects of piles driven in

chalk using three material zones of distinct physical and mechanical properties. Pedone et al. (2023) and Kontoe et al. (2025) showed how detailed considerations of these chalk zones are essential to the representative modelling of laterally loaded piles in chalk. Lovera (2019) similarly observed highly compacted crushed calcarenite annuli of the similar thickness to pile wall in pile driving into calcarenite and demonstrated how this crushed rock layer can be incorporated in the simplified 1-D modelling with p-y springs in series and 3D FE modelling of lateral pile tests. Installation effects also play significant roles in the analysis of axially loaded piles. Wen et al. (2023, 2024) incorporated distinct chalk zones in their load transfer ("t-z") analytical models and FE numerical models. Bateman & Crispin (2020) proposed theoretical "t-z" curves for piles in radially inhomogeneous soils with explicit modelling of installation effects.

Noting the congruent mechanical behaviour between silt-sized chalk and sand-sized calcarenite, this study explores the feasibility and applicability of a generalised 3D FE-based modelling framework for laterally loaded piles with explicit considerations of installation effects. The work draws on the earlier numerical studies by Pedone et al. (2023) and Kontoe et al. (2025) and employs simplified constitutive models with input parameters that can be readily calibrated from routine laboratory tests on intact and fully de-structured rock materials. The paper considers driven pile tests in: (i) low- to medium-density CIRIA Grade B2/B3 chalk at St Nicholas-at-Wade (Kent, UK) under the Wind Support (Ciavaglia et al., 2017), the ALPACA and ALPACA Plus (McAdam et al., 2024) campaigns; (ii) fine- to medium-grained calcarenite at Gouvieux (France) site (Lovera, 2019; Palix & Lovera, 2022).

2 MODELLING APPROACH AND INPUT DATA

2.1 *Driven pile tests in chalk and calcarenite*

Table 1 summarises the pile and rock conditions of the monotonic lateral pile tests reported by Ciavaglia et al. (2017), McAdam et al. (2024) and Lovera (2019). Other laterally loaded piles in these campaigns were either installed by other methods or experienced multi-staged monotonic or cyclic loading; these tests were therefore not considered in this numerical study.

Table 1. Summary of pile geometries and rock conditions.

Campaign	Rock type	Pile name	D (m)	L (m)	t_w (mm)
Wind Support	*Low- to medium-density chalk*	Pile 3	0.762	4.0	44.5
ALPACA & ALPACA Plus		LD12/13	0.508	3.05	20.6
		LD06/11	0.508	10.16	20.6
		TP2	1.2	7.32	25.0
Gouvieux	*Fine- to medium-grained calcarenite*	Pile 5	1.2	3.2	35.0
		Pile 7	0.762	2.7	35.0
		Pile 9	0.762	2.0	35.0

2.2 *Modelling of pile installation effects*

Installation effects were considered by incorporating new Zones: (A) remoulded and usually highly compacted rock, (B) rock with recent fracturing and reduced grading or quality, and (C) in-situ rock with old fractures and original quality, as illustrated schematically in Figure 2.

The thickness of the remoulded and compacted Zone A was assumed to be approximately equal to pile wall thickness (t_w), as observed in-situ by Buckley et al. (2018) and Vinck et al. (2025) for chalk and by Lovera (2019) for calcarenite. The thickness and characteristics of Zone B could vary substantially with rock properties, pile geometries, and/or installation method and energy. Pedone et al. (2023) assumed a fractured zone B thickness of ≈5 times of pile wall thickness. Vinck et al. (2025) found that Zone B scales radially with pile diameter (D) and wall thickness and proposed a refined Equation (1) for the radial distance (r_b) from the pile shaft to the outer Zone B boundary. This Equation was applied in the pile test cases where direct measurement or close inspection of rock zone divisions was unavailable in-situ. Greater uncertainties are expected in these cases. A fractured zone beneath pile tip that extends to a depth of approximately 5% of embedded length was considered in the models, following Wen et al. (2024).

$$r_b = 0.14 \times D + 6.1 \times t_w \quad (1)$$

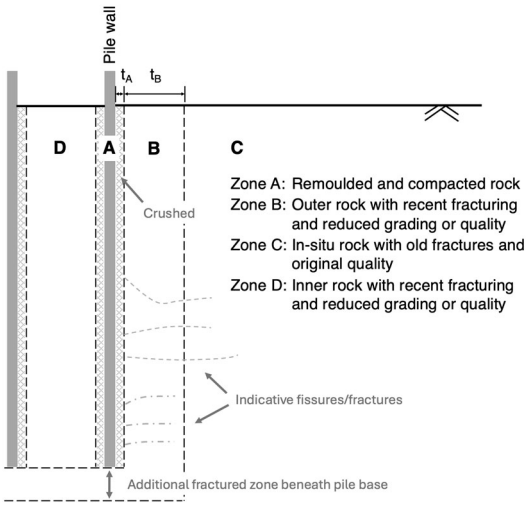

Figure 2. Schematic representation of rock zones created by pile driving (adopted from Buckley et al. (2018) and Vinck et al. (2025)).

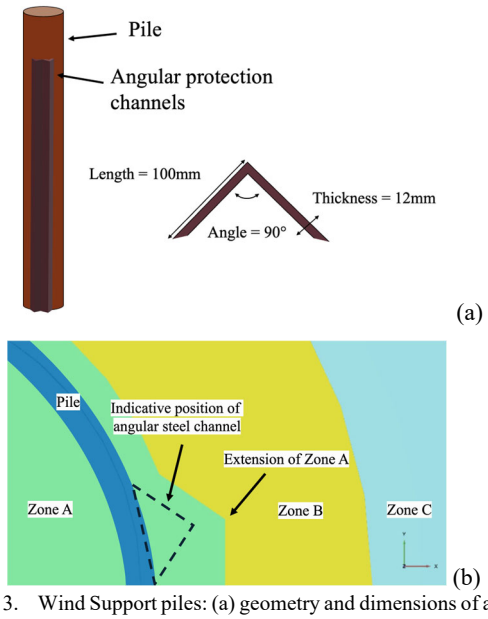

Figure 3. Wind Support piles: (a) geometry and dimensions of angular steel channels; (b) schematic chalk zone divisions applied in the model.

Some of the Wind Support piles had angular steel channels welded to their exteriors to protect the vibrating wire strain gauges deployed along the direction of lateral loading (Figure 3(a)). This modification increased the disturbance to the surrounding chalk during pile installation and created additional

fracturing, which was considered explicitly in the modelling. Zone A was extended to encompass the areas where the channels were located, assuming they created layers of puttified chalk with a thickness of t_w (Figure 3(b)). Rather than modelling installation disturbance around each triangular channel, a simplification was made by representing the additional Zone A as a single trapezoidal region surrounding both channels. The angular steel channels were not explicitly modelled as their influence on bending stiffness was negligible.

2.3 *Material properties and modelling parameters*

Linear elastic-perfectly plastic Mohr-Coulomb model was used for all zones of chalk or calcarenite. The key input parameters are summarised in Table 2. The chalk parameters were largely adapted from Pedone et al. (2023) and Wen et al. (2024) with adjustments to account for the differences in the constitutive models employed. Lower bound, constant, shear stiffness (G) values were adopted without considering any degradation with shear strain and variation against depth or in-situ stress. The effective strength parameters were calibrated from low and high pressure triaxial tests (Vinck et al., 2024; Liu et al., 2023), enabling detailed characterisation of chalk's yielding stresses and peak, post-rupture and ultimate strength (see Figure 1). A factored cohesion (c') of 159 kPa was used for chalk Zones B and C that represents the material's post-rupture strength, neglecting any pre-peak yielding and post-peak brittleness. Following Pedone et al. (2023), a shear resistance angle (ϕ') of 23.9° that represented the chalk's peak strength was also attempted and results are employed for comparison, as discussed later.

Table 2. Stiffness and strength parameters adopted in the analyses.

Chalk	G (MPa)	ν	c' (kPa)	ϕ' (°)
Zone A	500	0.2	3	31.5
Zone B	30	0.2	159	29
Zone C	250	0.2	159	29/23.9*
Calcarenite	**G (MPa)**	**ν**	**c' (kPa)**	**ϕ' (°)**
Zone A	4000	0.3	5	32
Zone B	240	0.3	350	29
Zone C	2000	0.3	350	29

Lovera (2019) reported uniaxial and triaxial compression tests on intact dry calcarenite samples from the Gouvieux test site, as well as direct shear tests on highly compacted crushed material collected post pile driving. The stiffness and strength parameters were further factored and approximated based on the rock quality designation (RQD) of rock cores, resulting in the input parameters summarised in Table 2.

The steel piles were modelled with linear elastic plate elements with Young's modulus of 210 GPa, Poisson's ratio (ν) of 0.28 and unit weight of 78.5 kN/m³. Centreline dimensions were used in the modelling with the plate elements representing pile diameter minus one wall thickness. No attempt was made to model the pile as elasto-plastic material and account for pile plasticity as the applied lateral loads had prevented structural yielding in most cases; see further discussions later.

3 FINITE ELEMENT MODELLING

3.1 *Geometry and boundary conditions*

Finite element analyses were performed using Plaxis 3D V2024.2.0 (Bentley Systems, 2024a). To reduce computational effort, half model was employed due to symmetry. Figure 4 shows the mesh layout for pile LD12/LD13 with the soil domain being discretised into 16669 10-noded tetrahedral elements (Bentley Systems, 2024b). The three rock zones (A, B and C), whose thicknesses were discussed earlier, are indicated and the parameters in Table 2 applied. The internal fractured chalk zone D was not explicitly distinguished for simplicity, given the piles' relatively small diameters, and was assigned the same material properties as for Zone A. Model boundaries were sufficiently extended to avoid any boundary effects.

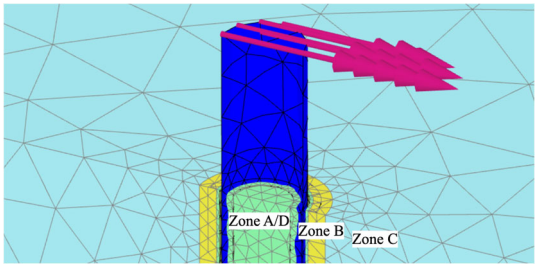

Figure 4. Discretised 3D FE model of ALPACA LD12/13.

Drained conditions were assumed for all models noting the relatively high in-situ permeabilities of the chalk mass at the SNW site and the dry conditions at the Gouvieux calcarenite site. The water tables in SNW varied between 5.5 m below ground level (BGL) for the ALPACA piles and 10 m BGL for the Wind Support pile. The water table at Gouvieux was reported lower than the bases of all tested piles. The initial stress states of the chalk and calcarenite were applied by assuming a K_0 value of 0.51 ($K_0 = 1 - \sin(\varphi')$). No attempt was made to reproduce any stress regime induced by pile installation.

External and internal pile shaft-rock interaction was modelled with zero-thickness interface elements with elastic interface normal and shear stiffness values (K_n and K_s) of 2.5×10^6 kN/m³ and 3.05×10^5 kN/m³ respectively for the chalk models, following Wen et al. (2024). Higher K_n and K_s values of 2.0×10^7 kN/m³ and 2.4×10^6 kN/m³ were applied for calcarenite, which were scaled proportionally from those applied for chalk noting calcarenite's higher shear moduli. A moderately conservative interface strength reduction factor (R_{inter}) of 0.7 (Murali et al., 2024) was applied in the calcarenite cases to capture more realistic load transfer mechanisms.

3.2 *Calculation phases*

Four main calculation phases were defined in the Plaxis 3D models, including: (i) establishing geostatic conditions in the ground, (ii) excavating the soil within the pile radius, (iii) activating the piles and rock zones to simulate pile installation effects, and (iv) applying displacement-controlled lateral loads at the loading elevations until ground level displacement reached 0.1D.

3.3 *Interpretation of bending moments*

Bending moments were calculated from modelling results by prescribing displacements corresponding to specific load levels. Axial force at nodal pairs were used to compute local bending moment contributions based on tributary areas and projected distances. Total moment at each elevation was obtained by summing and doubling these contributions to account for model symmetry. This process was repeated across multiple depths to generate moment profiles along full length.

4 RESULTS AND DISCUSSION

4.1 *Pile tests in low- to medium-density chalk (SNW)*

The computed load-displacement responses and bending moment profiles for the chalk cases were compared with field measurements in Figure 5 and Figure 6 respectively. The

employed simplified constitutive model yielded broadly good agreements between the modelled and measured results, noting the variations in the paired load tests. Good match was obtained for Wind Support Pile 3 for which irregular geometries of the welded protection channels were modelled explicitly. The initial stiffnesses of piles LD12/13 were well reproduced, although the ultimate capacity was overestimated. As expected, the predicted ultimate capacities made with the lower shear resistance angle of 23.9° were consistently lower but the initial stiffnesses appear largely unaffected. The bending moment profiles demonstrate clear patterns distinguishing slender and rigid piles, but the predictions made with the model inputs in Table 2 do not seem to indicate any consistent bias. Quality of match is quantified and discussed in a later Table 3.

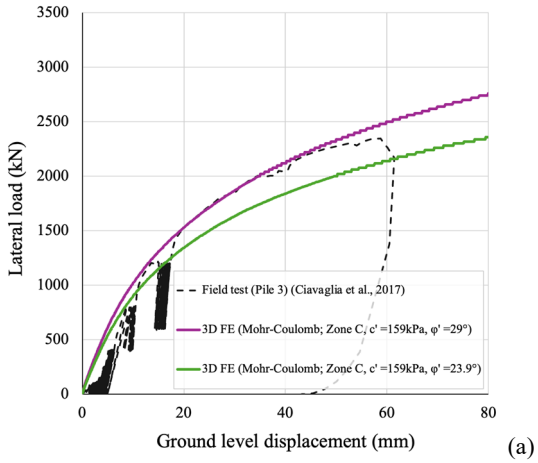

(a)

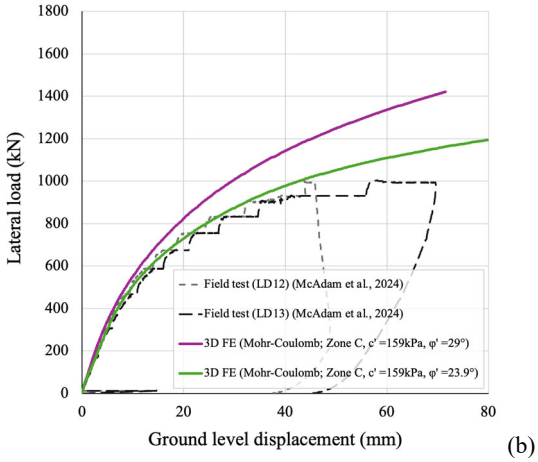

(b)

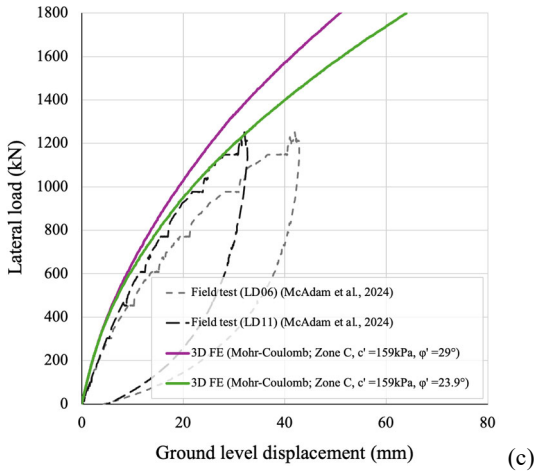

(c)

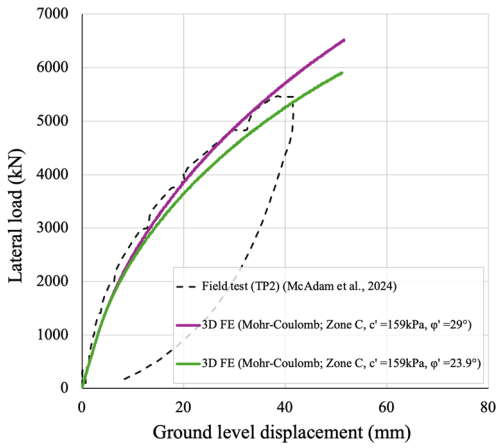

(d)

Figure 5. Measured and predicted load-displacement response for: (a) Wind Support Pile 3; (b) ALPACA Piles LD12/13; (c) ALPACA Piles LD06/11 and (d) ALPACA Plus Pile TP2.

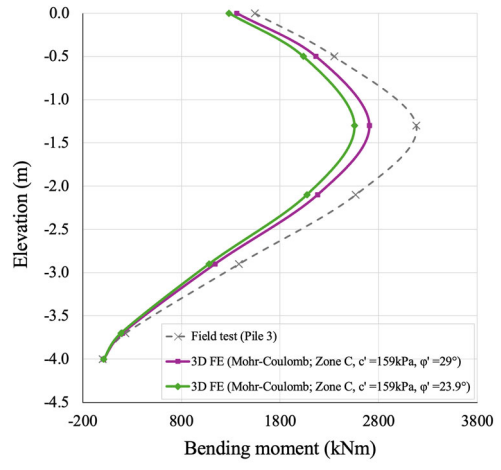

(a)

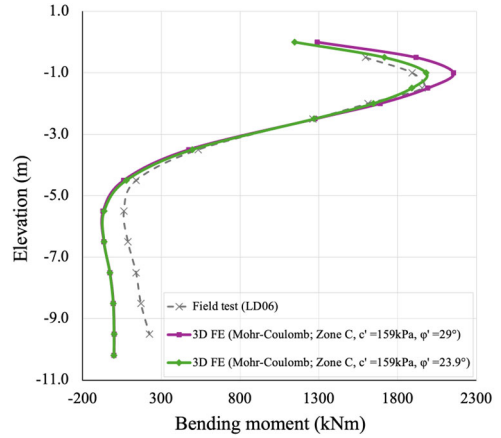

(b)

Figure 6. Measured and predicted bending moment profiles for: (a) Wind Support Pile 3 and (b) ALPACA Pile LD06 at ground level displacements of 40 mm and 60 mm, respectively.

4.2 *Pile tests in calcarenite (Gouvieux)*

Figure 7 compares the load-displacement curves for the Gouvieux piles in calcarenite. The field experiments reached relatively small displacements, introducing uncertainties in characterising the piles' ultimate capacities. The predictions capture broadly the lateral capacities observed in the tests, although the stiffness of Pile 5 appears to be overestimated. No high-quality strain gauge data was available from the field testing to facilitate further comparisons in bending moment

profiles. The difficulties in accurately modelling the load-displacement response using a continuum approach may be partly attributed to the occurrence of radial ground cracks after pile installation and lateral loading, as observed by Lovera (2019). Further parametric studies with advanced constitutive models may be undertaken to further explore these factors.

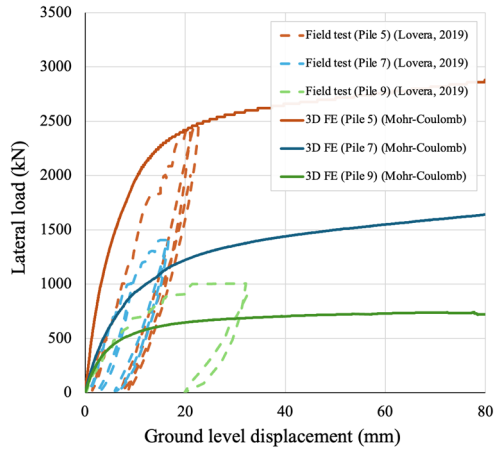

Figure 7. Measured and predicted load-displacement response for Gouvieux Piles 5, 7 and 9.

4.3 *Assessment of matching quality*

The accuracy metric defined by Burd et al. (2020) was employed to assess the quality of matching between the field experiments and model predictions. Matching quality was assessed using Equation (2) over small ground level displacement (GLD) of ≤ D/10,000 (η_{sd}) and over large GLD of ≤ D/10 (η_{ult}). The maximum field displacement ranges were assessed in cases where GLD did not reach D/10.

$$\eta = \frac{A_{ref} - A_{diff}}{A_{ref}} \quad (2)$$

Table 3 presents the accuracy metrics for each pile for the load-displacement trends and bending moment profiles. Field measurements at very small displacements were subject to greater uncertainties with generally lower quality data, particularly with the Gouvieux piles 5, 7 and 9 for which negative or low η_{sd} values were obtained.

Table 3. Accuracy metric (η) values for load-displacement responses and bending moment profiles.

Pile	Load-displacement		Bending moments	
	η_{sd}	η_{ult}	GLD (mm)	η_{GLD}
LD12	0.96	0.84	40	0.88
LD13	0.77	0.78	60	0.65
LD06	0.86	0.66	40	0.96
LD11	0.82	0.87	20	0.95
TP2	0.90	0.97	40	0.85
Pile 3	0.59	0.97	40	0.87
Pile 5	-1.25	0.75	/	
Pile 7	-0.97	0.89	/	
Pile 9	0.16	0.61	/	

4.4 *Extraction of soil reaction curves*

The mobilised lateral loads (p) normalised by pile diameter (D) and rock shear strength (S_u) are plotted for the selected Wind Support and ALPACA piles in chalk and Gouvieux pile in calcarenite at shallow elevations, as shown in Figure 9. An average triaxial shear strength of 1350 kPa was adopted for chalk and 3000 kPa (half of peak uniaxial compression strength) for calcarenite. Also plotted for comparison is the p-y curve proposed by McAdam et al. (2024). The ultimate $p_u/(D\times S_u)$ extracted from the chalk analyses spanned a range of 0.9-2.9, with an average value close to 1.9 for depths up to 1.5 mBGL. The calcarenite cases indicated a lower yet comparable $p_u/(D\times S_u)$ range of 0.6-2.3. Xu et al. (2025) present in parallel a critical appraisal of p-y models for laterally loaded piles in weak rocks, highlighting the distinct rock-pile interaction mechanisms at the local and global scales.

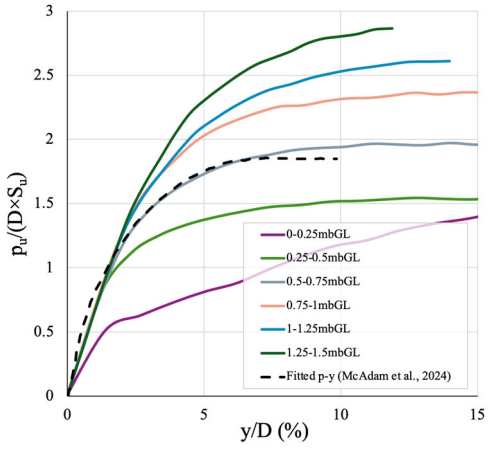

(a)

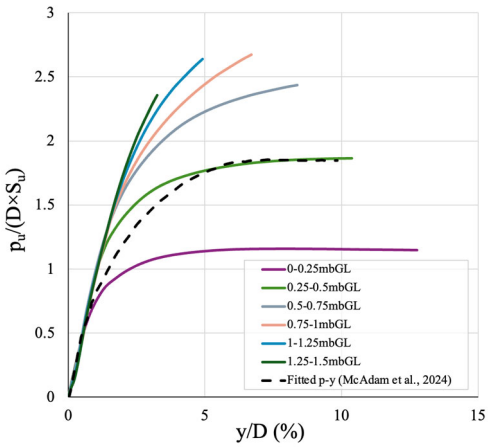

(b)

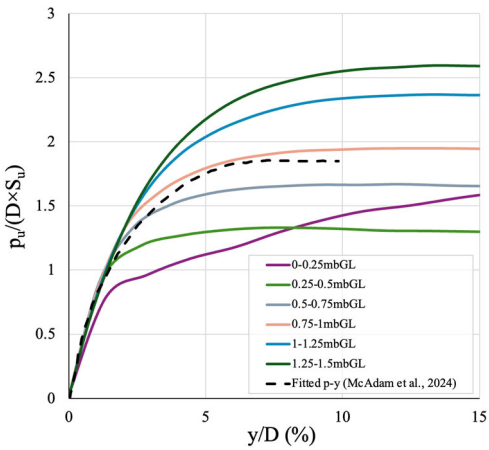

(c)

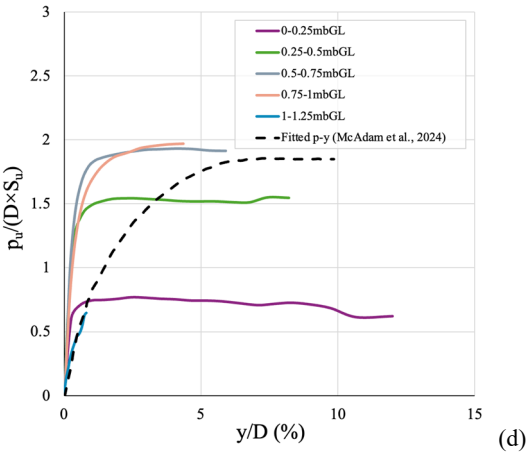

Figure 8. Normalised p-y curves in comparison with the proposal by McAdam et al. (2024) for: (a) Wind Support Pile 3; (b) ALPACA Piles LD12/13; (c) ALPACA Plus Pile TP2 and (d) Gouvieux Pile 9.

4.5 *Structural yielding*

Structural yielding is particularly concerning when pile interacts against rocks. Stresses in pile walls were inspected for all cases. The yield stresses in Piles LD06/11 were slightly exceeded when loaded to 40 mm GLD at which the piles were subsequently unloaded to avoid any significant steel yielding. Pile 7 was also estimated to yield at GLD of 40 mm, although the test was halted as other failure criteria were met. The computed bending stress maxima found for the other piles in chalk and calcarenite were invariably below the respective steel yield strengths, including for the large diameters ALPACA Plus TP2 and Gouvieux Pile 5, with stress mobilisation ratios ranging from 0.36 to 0.89 at 40 mm GLD. The results confirmed the piles behaved elastically throughout loading.

5 CONCLUSIONS

This numerical study aimed at demonstrating the feasibility and applicability of a generalised 3D FE-based modelling framework for laterally loaded piles with explicit consideration of installation effects, focusing on low- to medium-density chalk and fine- to medium-grained calcarenite encountered in benchmarking field pile testing as part of several joint industry projects. The main conclusions are as follows:

- Pile installation effects on lateral pile loading response were captured effectively by incorporating concentric rock zones with distinct mechanical properties and thicknesses. The FE analyses also enabled direct modelling and consideration of irregular pile geometries caused by welded protection channels on the Wind Support piles.
- The FE analyses performed with simplified constitutive models and input parameters that capture the peak, post-rupture and ultimate strength characteristics of chalk and calcarenite yielded reasonably good matches with field measurements of load-displacement and bending moment.
- Local soil reaction p-y curves extracted from the analyses aligned well with the proposal by McAdam et al. but showed wider spreads and greater variations with depth.

6 ACKNOWLEDGEMENTS

The reported study formed part of the first Author's research project undertaken at the University of Bristol. The support by Dr Liz Holcombe and Professors Dimitris Karamitros and Erdin Ibraim is acknowledged. The second Author thanks gratefully the insightful discussions with the ALPACA and ALPHA research teams, particularly Professors Richard Jardine and Stavroula Kontoe and Drs Giuseppe Pedone and Ken Vinck of the pile tests in chalk, and with Elisabeth Palix of EDF Renewables (Paris, France) of the Gouvieux pile tests.

REFERENCES

Bentley Systems, 2024a. PLAXIS 3D, Version 2024.2.0. *Bentley Systems, Inc*.

Bentley Systems, 2024b. PLAXIS 3D Reference Manual. *Bentley Systems, Inc*.

Buckley, R.M., Jardine, R.J., Kontoe, S., Parker, D. and Schroeder, F.C. 2018. Ageing and cyclic behaviour of axially loaded piles driven in chalk. *Géotechnique*, 68(2), 146-161.

Burd, H.J., Abadie, C.N., Byrne, B.W., Houlsby, G.T., Martin, C.M., McAdam, R.A., Jardine, R.J., Pedro, A.M.G., Potts, D.M., Taborda, D.M.G., Zdravković, L. and Pacheco Andrade, M. 2020. Application of the PISA design model to monopiles embedded in layered soils. *Géotechnique*, 70(11), 1067-1082.

Ciavaglia, F., Diambra, A. and Carey, J. 2017. Monotonic and cyclic lateral tests on driven piles in Chalk. *Geotechnical Engineering*, 353-366.

Cuccovillo, T. and Coop, M.R. 1999. On the mechanics of structured sands. *Géotechnique*, 49(6), 741-760.

Kontoe, S., Bellument, E., Pedone, G. and Jardine, R.J. 2025. 3D FE analysis of laterally loaded piles driven in chalk. *Proc. 5th International Symposium on Frontiers in Offshore Geotechnics*, 1288-1293.

Lagioia, R. and Nova, R. 1995. An experimental and theoretical study of the behaviour of a calcarenite in triaxial compression. *Géotechnique*, 45(4), 633-648.

Lovera, A. 2019. Cyclic lateral design for offshore monopiles in weak rocks. Doctoral thesis, Université Paris-Est.

Liu, T., Ferreira, P.M., Vinck, K., Coop, M.R., Jardine, R.J. and Kontoe, S. 2023. The behaviour of a low-to medium-density chalk under a wide range of pressure conditions. *Soils and Foundations*, *63*(1), 101268.

McAdam, R.A., Buckley, R.M., Schranz, F., Byrne, B.W., Jardine, R.J., Kontoe, S., Liu, T., Vinck, K. and Crispin, J. 2024. Monotonic and cyclic lateral loading of piles in low- to medium-density chalk. Ahead of Print in *Géotechnique*.

Murali, A. K., Haque, A. and Bui, H.H., 2024. Advancing Rock-Socketed Pile Design with a Unified Interface Shear Strength Framework for Soft Rocks. *Rock Mechanics & Engineering,* 57, 7253-7269.

Palix, E. and Lovera, A. 2020. Field testing for monopile to be installed in weak carbonated rock. *Proc. 4th International Symposium on Frontiers in Offshore Geotechnics*, 1086-1995.

Palix, E. 2025. Offshore wind turbine foundations on rocky formations – The French experience. *Proc. 5th International Symposium on Frontiers in Offshore Geotechnics*, 127-144.

Pedone, G., Kontoe, S., Zdravković, L., Jardine, R.J., Vinck, K. and Liu, T. 2023. Numerical modelling of laterally loaded piles driven in low-to-medium density fractured chalk. *Computers and Geotechnics*, 156, 105252.

Randolph, M., 2020. Keynote Lecture: Considerations in the Design of Piles in Soft Rock. In: Duc Long, P., Dung, N. (eds) Geotechnics for Sustainable Infrastructure Development. *Lecture Notes in Civil Engineering* 62, Singapore: Springer.

Vinck, K., Liu, T., Jardine, R.J., Lawerence, J.A. and Buckley, R.M. 2025. Characterising the damage developed around piles by percussive driving in low-to-medium density chalk. *Proc. 5th International Symposium on Frontiers in Offshore Geotechnics*, 1290-1395.

Wen, K., Kontoe, S., Jardine, R.J. and Liu, T. 2023. An Axial Load Transfer Model for Piles Driven in Chalk. *Journal of Geotechnical and Geoenvironmental Engineering*, 149(11), 1090-0241.

Wen, K., Kontoe, S., Jardine, R.J. and Liu, T. 2024. Finite element modelling of pipe piles driven in low-to-medium density chalk under monotonic axial loading. *Computers and Geotechnics*, 172, 106458.

Xu, Z., Diambra, A., Liu, T. and Ge, B. 2025. A critical appraisal of p-y models for laterally loaded piles in weak rocks. In *21st International Conference on Soil Mechanics and Geotechnical Engineering, Vienna*.